

Synthesis of a Sustainable and Bisphenol A-Free Epoxy Resin Based on Sorbic Acid and Characterization of the Cured Thermoset

Jonas M. Breitsameter, Nikita Reinhardt, Matthias Feigel, Olaf Hinrichsen, Klaus Drechsler, and Bernhard Rieger*

In the present study, an epoxy compound, 1,2-epoxy-6-methyl-triglycidyl-3,4,5-cyclohexanetricarboxylate (EGCHC) synthesized from sorbic acid, maleic anhydride, and allyl alcohol is proposed. Using commodity chemicals, a bio-based carbon content of 68.4 % for the EGCHC resin is achieved. When cured with amine hardeners, the high oxirane content of EGCHC forms stiff cross-linked networks with strong mechanical and thermal properties. The characterization of the epoxy specimens showed that EGCHC can compete with conventional epoxy resins such as DGEBA. A maximum stiffness of 3965 MPa, tensile strength of 76 MPa, and T_g of 130 °C can be obtained by curing EGCHC with isophorone diamine (IPD). The cured resin showed to be decomposable under mild conditions due to the ester bonds. The solid material properties of EGCHC expose its potential as a promising bisphenol A, and epichlorohydrine free alternative to conventional petroleum-based epoxies with an overall high bio-based carbon content.

Over the years they became more and more important: because of their versatile application in coatings for electronics, floor coverings, multi-component adhesives, or as a matrix in fiber reinforced composite materials, epoxy resins are of industrial interest.^[2-5] About 90% of the epoxy thermoset is derived from diglycidyl ether of bisphenol A (DGEBA).^[6] DGEBA shows after curing with a suitable curing agent excellent mechanical properties and high resistances against chemicals or heat due to the aromatic structure and the interactions resulting from this.^[5,7,8] However, there are concerns linked with bisphenol A including the classification as endocrine disruptor^[9-14] and the toxicity of reagents which are used to produce DGEBA such as epichlorohydrine (ECH).^[15] As a result, there is a great motivation to find alternative materials.

1. Introduction


By discovering the oxidation of unsaturated compounds in 1909, Prilezhaev also initiated the development of epoxy resins.^[1]

Research mostly concentrated on finding bio-based building blocks for epoxy resins. Consequently, biomolecules of all kinds were identified as possible precursors. As can be seen in **Table 1**, most promising candidates are phenolic structures such as eugenol, cinnamic acid, vanillin or lignin fragments because of their structural similarity to BPA and high aromaticity.^[16-26] These biomolecules usually are reacted with ECH to form the glycidyl ether.^[27-31] The same etherification reaction can be applied on bio-based aliphatic polyols like sugars, pentaerythritol, or glycerin.^[32-35] The biggest drawback of this approach is the need of ECH for the introduction of epoxy groups and the concerns coming with it discussed earlier. To decrease the environmental impact of ECH the traditional synthesis starting from mineral oil nowadays is more and more substituted by glycerin as renewable feedstock. ECH is readily available in an industrial scale as a bio-based product with a share of 20% in the European market of bio-based platform chemicals (2020).^[36] This surely diminishes the carbon footprint of the chemical but not the environmental impact.^[37,38] Compared with phenolic structures, aliphatic heterocycles such as sugars can not compete with the thermal and mechanical properties of aromatic compounds in most cases due to structural disadvantages. As an example, triglycidyl eugenol derivative cured with isophorone diamine (IPD) shows a glass transition temperature (T_g) of 174 °C^[27] while the sugar-based isosorbide epoxy reaches a T_g of 73 °C.^[34] A chemically different approach is pursued with unsaturated vegetable oils. Here, the

J. M. Breitsameter, B. Rieger
Wacker-Chair of Macromolecular Chemistry
TUM School of Natural Sciences
Technical University of Munich
85748, Lichtenbergstr. 4 Garching, Germany
E-mail: rieger@tum.de

N. Reinhardt, K. Drechsler
Chair of Carbon Composites
TUM School of Engineering and Design
Technical University of Munich
85748, Boltzmannstr. 15 Garching, Germany

M. Feigel, O. Hinrichsen
Chair I of Technical Chemistry
TUM School of Natural Sciences
Technical University of Munich
D-85748, Lichtenbergstr. 4 Garching, Germany

 The ORCID identification number(s) for the author(s) of this article can be found under <https://doi.org/10.1002/mame.202300068>

© 2023 The Authors. Macromolecular Materials and Engineering published by Wiley-VCH GmbH. This is an open access article under the terms of the Creative Commons Attribution License, which permits use, distribution and reproduction in any medium, provided the original work is properly cited.

DOI: 10.1002/mame.202300068

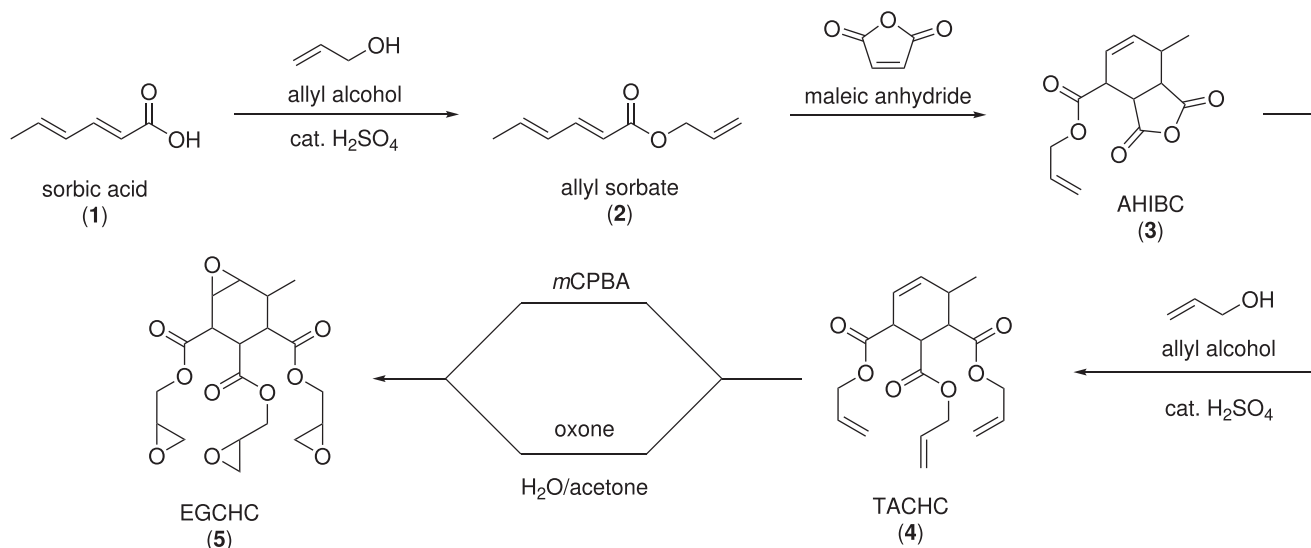


Figure 1. Synthesis route toward the epoxy monomer compound EGCHC (5) starting from the allylation of sorbic acid (1) which is then reacted with maleic anhydride in a Diels–Alder cycloaddition. After the allylation of the anhydride moiety of (4) the double bonds are epoxidized by the use of *m*CPBA or oxone®.

Table 1. A selection of bio-based epoxy thermoset from the literature based on the given biomolecule. Besides of ELO (epoxidized linseed oil) are all resins the glycidyl ether of the biomolecule. Abbreviations of hardeners: MNA = methyl nadic anhydride, DETDA = diethylene toluene tetramine (aromatic), D230 = Jeffamine D230 linear polyetheramine, TETA = triethylenetetramine, MTHPA = methyltetrahydrophthalic anhydride, TA = tannic acid (aromatic).

Category	Based on	Hardener	T_g °C ⁻¹
Cycloaliphatic	Isosorbide	IPD	73 ^[33]
Cycloaliphatic	Glucofuranoside	DETDA	178 ^[32]
Aliphatic	Glycerol	DETDA	65 ^[32]
Aliphatic	Pentaerythritol	DETA	98 ^[32]
Aromatic	Eugenol	IPD	174 ^[27]
Aromatic	Cinnamic acid	MNA	117 ^[29]
Aromatic	Vanillin	D230	106 ^[16]
Aromatic	Lignin	anhydride	94 ^[28]
EVO	Linseed oil (ELO)	TETA	54 ^[46]
EVO	Linseed oil (ELO)	MTHPA	145 ^[46]
EVO	Linseed oil (ELO)	TA	146 ^[43]

double bonds embedded in long hydrocarbon chains can be easily epoxidized by peracids but show less reactivity during the curing process and the cured resins only show relatively low T_g .^[39–45]

In this study, we report a synthetic route toward a multifunctional epoxy resin whose components are directly bio-available or can be synthesized from biomolecules. As shown in **Figure 1**, the synthesis starts from bio-available sorbic acid. Allyl alcohol used in condensation reactions twice can be derived from glycerin and obviates the use of ECH. Maleic anhydride as well can be obtained indirectly from carbohydrates. Taking a conservative approach, a bio-based carbon content of 68.4% can be reached for

EGCHC resin as described in Section 3.7. Therefore, a largely bio-based, and BPA and ECH-free alternative to the traditional and petroleum-based DGEBA could be found.

EGCHC resin was cured with two different hardeners, T403 and IPD in order to investigate the impact of the chemical structure of the curing agent on the properties of the EGCHC-based epoxy. T403 and IPD are common amine-based curing agents that are used industrially in high-performance epoxy systems. Their use in common DGEBA-based epoxies are well-described in the literature.^[47–51] Reference samples were also prepared with DGEBA cured with T403 and IPD in order to compare the thermo-mechanical properties, mechanical properties and the thermal stability of EGCHC with DGEBA, one of the most used epoxy resin.

2. Experimental Section

2.1. Materials

All chemicals were purchased from Sigma–Aldrich unless otherwise noted and were used as received: Sorbic acid ($\geq 99.0\%$), allyl alcohol ($\geq 98.5\%$), maleic anhydride ($\geq 99.0\%$), sulfuric acid (ACS reagent, 95.0–98.0 %), toluene (ACS reagent, $\geq 99.5\%$), diethyl ether ($\geq 99.9\%$, suitable for HPLC, inhibitor free) 3-chloroperbenzoic acid (*m*CPBA, $\geq 77\%$), oxone (>4.0 % active oxygen basis), methylene chloride (suitable for HPLC, $\geq 99.8\%$, contains 40–150 ppm amylene as stabilizer), potassium carbonate (Grüssing, K_2CO_3 , $\geq 99.5\%$), sodium sulfate (Grüssing, Na_2SO_4 , 99 %, anhydrous), sodium bicarbonate (Grüssing, $NaHCO_3$, $\geq 99.5\%$), sodium hydroxide (Fischer scientific, NaOH, $\geq 98.0\%$ Baker analyzed), bisphenol A-diglycidyl-ether (Epoxide equivalent weight: 172–176), Jeffamine T403 (Huntsman Holland B.V.), isophoron diamine (mixed isomers, $\geq 99\%$).

2.2. Synthesis of EGCHC Epoxy Monomer

2.2.1. Allylation of Sorbic Acid

Sorbic acid (50 g, 445.9 mmol) was dissolved in allyl alcohol (200 mL). After the addition of a catalytic amount of H₂SO₄ (0.5 vol.%, 1.0 mL) the mixture was stirred under reflux for 24 h. After the reaction had cooled to room temperature it was neutralized by the addition of saturated sodium bicarbonate solution and the product was extracted with diethyl ether (3 × 200 mL). The combined organic layers were washed with saturated sodium chloride (200 mL) and dried with anhydrous sodium sulfate. After filtration, the solvent was removed *in vacuo* and the crude product was purified by distillation (82 °C, 8 mbar). The product allylsorbate (2) was obtained in form of a colorless liquid (55.6 g, 82 %). ¹H-NMR (400 MHz, chloroform-d, ppm): δ 7.27 (m, H4), 6.17 (m, H3), 5.95 (m, H8), 5.80 (d, J = 15.4 Hz, H2), 5.27 (m, H5/H9), 4.65 (m, H7), 1.86 (d, J = 5.7 Hz, H1). ¹³C-NMR (100 MHz, chloroform-d, ppm): 167.00 (C6), 145.46 (C4), 139.65 (C2), 132.54 (C8), 129.88 (C3), 118.37 (C5), 118.07 (C9), 64.99 (C7), 18.75 (C1).

2.2.2. Diels–Alder Reaction of Allyl Sorbate and Maleic Anhydride

Maleic anhydride (26.3 g, 268.08 mmol, 1.02 eq.) was dissolved in toluene (26 mL, 10 M solution) and heated to reflux. Allyl sorbate (40 g, 262.82 mmol, 1.0 eq.) was added under vigorous stirring. Since the reaction was strongly exothermic, heating of the mixture was interrupted for several minutes when exceeding 140 °C in the vessel. Reaction progress was monitored by ¹H-NMR and stopped after full conversion which was reached within 2.5 h. The crude product crystallizes by cooling down the reaction mixture to 0 °C and the solid was washed with cold methanol. After drying *in vacuo*, the product allyl 7-methyl-1,3-dioxo-1,3,3a,4,7,7a-hexahydroisobenzofuran-4-carboxylate (AHIBC, 3) was obtained as a white, crystalline solid (56.4 g, 84 %). ¹H-NMR (400 MHz, chloroform-d, ppm): δ 6.47 (1H, dt, J = 9.49, 3.32 Hz, H3), 5.98 (1H, m, J = 16.61, 10.38, 5.98 Hz, H12), 5.86 (1H, dt, J = 9.40, 3.24 Hz, H2), 5.4 – 5.2 (2H, m, H13), 4.76 (2H, dt, J = 6.09, 1.32 Hz, H11), 4.02 (1H, dd, J = 9.78, 5.55 Hz, H5), 3.39 (1H, dd, J = 9.79, 7.82 Hz, H6), 3.19 (1H, m, H4), 2.47 (1H, m, H1), 1.43 (3H, d, J = 7.34 Hz, H9). ¹³C-NMR (100 MHz, chloroform-d, ppm): 171.3 (C7), 170.3 (C8), 169.2 (C10), 134.8 (C2), 131.7 (C12), 127.0 (C3), 119.1 (C13), 66.4 (C11), 44.6 and 44.5 (C5 and C6), 40.1 (C4), 30.8 (C3), 16.4 (C9). ATR-IR $\tilde{\nu}_{max}$ 2975, 2938, 2881, 1846, 1768, 1716, 1648, 1455, 1426, 1391, 1363, 1329, 1302, 1260, 1227, 1196, 1141, 1084, 1066, 1052, 1030, 950, 922, 904, 884, 817, 781, 747, 712 cm⁻¹. EA Found: C, 62.08; H, 5.63. C₁₃H₁₄O₅ requires C, 62.39; H, 5.64 %. HRMS (ESI) calculated C₁₃H₁₅O₅ [M + H⁺] 251.0914, found 251.0912. M.p. 88.6 °C.

2.2.3. Allylation of AHIBC

AHIBC (40 g, 159.84 mmol) was dissolved in allyl alcohol (190 mL). After the addition of a catalytic amount of H₂SO₄ (0.5 vol.%, 0.9 mL), the mixture was stirred under reflux and the reaction progress was monitored by ¹H-NMR. The reaction usually was complete within 24 h. After the mixture had cooled to

room temperature it was neutralized by the addition of a saturated sodium bicarbonate solution and the product was extracted with diethyl ether (3 × 200 mL). The combined organic layers were washed with saturated sodium chloride (200 mL) and dried over anhydrous sodium sulfate. After filtration, the solvent was removed *in vacuo*. The crude product was purified by column chromatography (1:6 EtOAc/hexanes). The product triallyl-6-methylcyclohex-4-ene-1,2,3-tricarboxylate (TACHC, 4) was obtained as a colorless oil (45.2 g, 81 %). ¹H-NMR (400 MHz, chloroform-d, ppm): δ 6.09 (1H, m, H3), 5.90 (3H, m, H12, H12', H12''), 5.65 (1H, m, H2), 5.38 – 5.16 (6H, m, H13, H13', H13''), 4.58 (6H, m, H11, H11', H11''), 3.55 (1H, m, H5), 3.45 (1H, m, H6), 3.11 (1H, m, H4), 2.64 (1H, m, H1), 1.06 (3H, d, J = 7.36 Hz, H9). ¹³C-NMR (100 MHz, chloroform-d, ppm): δ 171.8, 171.4 and 170.73 (C10, C7 and C8), 132.5, 132.4, 132.1, 132.0 (C12, C12', C12'' and C2), 122.9 (C3), 118.5, 118.4 and 118.4 (C13, C13', C13''), 65.8, 65.7 and 65.3 (C11, C11', C11''), 43.5 (C6), 42.3 and 42.1 (C4, C5), 32.2 (C1), 17.2 (C9). ATR-IR $\tilde{\nu}_{max}$ 3455, 2940, 2882, 1730, 1649, 1454, 1379, 1310, 1169, 1094, 1061, 911, 927, 833, 720 cm⁻¹. EA Found: C, 65.22; H, 6.88. C₁₉H₂₄O₆ requires C, 65.50; H, 6.94 %. HRMS (ESI) calculated C₁₉H₂₄O₆Na [M + Na⁺] 371.1471, found 371.1451.

2.2.4. Epoxidation of TACHC with mCPBA

To obtain EGCHC (5), 40 g (114.81 mmol, 1.0 eq.) of the TACHC (4) was reacted with 158.50 g mCPBA (918.5 mmol, 8 eq.) in DCM (500 mL) at room temperature. Reaction progress was monitored by ¹H-NMR and was usually completed within 48 h. The reaction mixture was then stirred over K₂CO₃ (200 g) to deactivate residual mCPBA and the resulting m-chlorobenzoic acid was separated by filtration. The organic phase was then washed with a sodium thiosulfate solution (300 mL, 10 wt.%), H₂O (200 mL), and brine (200 mL). After drying over sodium sulfate and removing the solvent *in vacuo* 1,2-epoxy-6-methyl-triglycidyl-3,4,5-cyclohexanetricarboxylate (EGCHC, 5) was obtained as a colorless viscous oil (36.9 g, 78 %). ¹H-NMR (400 MHz, chloroform-d, ppm): δ 4.45 – 4.0 (3H, m, H11, H11', H11''), 3.93 (1H, m, H3), 3.76 (3H, m, H11, H11', H11''), 3.35 (1H, m, H4), 3.28 (1H, m, H5), 3.13 (3H, m, H12, H12', H12''), 2.97 (1H, m, H2), 2.93 (1H, m, H6), 2.80 – 2.73 (3H, m, H13, H13', H13''), 2.60 – 2.54 (3H, m, H13, H13', H13''), 2.38 (1H, q, H1), 1.06 (3H, m, H9). ¹³C-NMR (100 MHz, chloroform-d, ppm): δ 172.6, 172.0 and 169.8 (C10, C7 and C8), 65.9 (C11, C11', C11''), 56.8 (C3), 53.6 (C2), 49.2 – 48.9 (C12, C12', C12''), 44.8 – 44.5 (C13, C13', C13''), 41.5 (C4), 40.9 (C6), 39.6 (C5), 30.9 (C1), 14.8 (C9). ATR-IR $\tilde{\nu}_{max}$ 2950, 1729, 1434, 1385, 1348, 1304, 1256, 1199, 1179, 1078, 1045, 1012, 940, 905, 840, 762, 738 cm⁻¹. EA Found: C, 55.12; H, 8.87. C₁₉H₂₄O₁₀ requires C, 55.12; H, 8.83 %. HRMS (ESI) calculated C₁₉H₂₄O₁₀Na [M + Na⁺] 435.1267, found 435.1249.

2.2.5. Epoxidation of TACHC with Oxone

0.943 g (2.71 mmol, 1.0 eq.) of TACHC was dissolved in acetone (200 mL). Sodiumbiscarbonate (37.5 g, 446.0 mmol, 165 eq.) was added suspended in 90 mL of water and added to the acetone-solution. The mixture was cooled in an ice bath and oxone (50.0 g,

Table 2. Mixing ratios for the EGCHC and DGEBA-based samples.

Sample	Resin [g]: Curing agent [g]	Molar ratio
EGCHC-IPD	2:0.842	1.0
EGCHC-T403	2:1.571	1.0
DGEBA-IPD	2:0.499	1.0
DGEBA-T403	2:0.950	1.0

Table 3. Curing conditions for the EGCHC and DGEBA-based samples.

Sample	Curing time + temperature	Post-curing time + temperature
EGCHC-IPD	30 min at 45 °C	30 min at 120 °C
EGCHC-T403	2 h at 60 °C	2 h at 100 °C
DGEBA-IPD	2 h at 60 °C	2 h at 160 °C
DGEBA-T403	3 h at 80 °C	2 h at 120 °C

81.2 mmol, 30 eq.) in H₂O (170 mL) was added drop wise over a period of 30 min. The reaction mixture was then stirred for three days at room temperature. After extraction with ethyl acetate (3 × 100 mL) the combined organic phases were washed with a saturated sodium chloride solution, dried over sodium sulfate, and the solvent was removed *in vacuo*. EGCHC (5) was obtained as a colorless viscous oil (0.338 g, 30.2 %). Spectral data as described for the epoxidation with *m*CPBA. The EEW was determined to be 107.7 g mol⁻¹ by titration following the procedure of EN ISO 3001 : 9000.

2.3. Preparation of Epoxy Samples

EGCHC and DGEBA-based epoxy samples were prepared as follows: 2 g of EGCHC or DGEBA and the according amount of curing agent (Table 2) were mixed in 20 mL screw cap vials with septum with a Classic Advanced Vortex Mixer (Velp Scientifica, Italy) at a speed of 30000 rpm for 1 min. The mixtures were degassed with vacuum for 3 min to remove air inclusions. The EGCHC-IPD mixture was degassed for 30 s only as it already sets after 4 min at room temperature. Then, the mixture was poured into the cavities of a silicone mold. For Dynamic Mechanical Analysis (DMA), the silicone mold had cavities with the dimensions 30 mm × 5 mm × 1 mm. For tensile testing, the silicone mold had cavities with the dimensions of the dogbone sample geometry 1BB from ISO 527-2 with a thickness of 1 mm and a total length of 30 mm. A glass plate coated with release agent was put on the silicone mold in order to ensure a flat surface of the epoxy samples. Finally, the mold was placed in an oven for curing (Table 3). After curing, the edges of the samples were wet-polished with sandpaper (grid size 500) for a smooth finish.

2.4. Nuclear Magnetic Resonance (NMR) Spectroscopy

¹H (400 MHz) and ¹³C (100 MHz) nuclear magnetic resonance experiments were conducted on a Bruker AV400 instrument in deuterated chloroform (Sigma–Aldrich, CDCl₃, 99.8 atom% D) or methylene chloride (Sigma–Aldrich, CD₂Cl₂, 99.9 atom% D) as

the solvent at a temperature of 294 K. Chemical shifts were referenced to the solvent proton resonance (CDCl₃: 7.26 ppm for ¹H-NMR, 77.2 ppm for ¹³C-NMR; CD₂Cl₂: 5.32 ppm for ¹H-NMR, 53.84 ppm for ¹³C-NMR).

2.5. Differential Scanning Calorimetry (DSC)

DSC measurements were conducted with a TA Instruments Q2000 differential scanning calorimeter under 25 mL min⁻¹ helium flow. 5 to 9 mg of the resin/curing agent mixtures were loaded inside a TZero aluminum pan from TA Instruments. Samples were cooled down at -50 °C and subjected to a heating rate of 10 K min⁻¹. The onset temperature of the curing enthalpy and the temperature of the maximum of the exothermic peak were determined with the software Universal Analysis.

2.6. Dynamic Mechanical Analysis (DMA)

DMA measurements were performed using a DMA Q800 (TA Instruments, US) under a nitrogen atmosphere with a film tension clamp. After mounting on the clamp, the specimens had a free length of about 18 mm. The samples were subjected to an oscillating tensile load with a frequency of 2 Hz, a static pre-load of 0.01 N, and a force profile of 125 %. The amplitude for the specimens cured with IPD was 3 and 2 μm for the samples cured with T403. During loading, the samples were first equilibrated at -20 °C for 5 min, then a temperature ramp of 2K min⁻¹ was applied. Three specimens were characterized for each epoxy system. The glass transition temperature *T*_g was identified as the temperature of the peak of the tan δ curve using the software Universal Analysis.

2.7. Tensile Testing

The dogbone samples were painted using an airbrush and a matte acrylic-based paint. A white base coat was applied to the region of interest and then a black speckle pattern was sprayed on top. The amount of paint applied was carefully minimized in order not to smear the underlying stress field. Tensile testing was performed with a universal testing machine Inspekt 100 (Hegewald & Peschke, Germany) equipped with screw clamps. The force was measured using a 500 N load cell. The Dogbones samples were tested at a constant loading speed of 0.125 mm min⁻¹. Five specimens were tested for each epoxy system. The average laboratory temperature and humidity during testing were 21.8 °C and 33 %. A VCXU-124M camera (Baumer, Germany) mounted on a telecentric lens VS-TCM1-130/S (VS Technology, Japan) captured the deformation on the specimens surface during testing. The recorded pictures were transferred to the Software GOM Correlate Professional 2020 and the tensile modulus was evaluated from the stress/strain curves in the elongation range between 0.05 and 0.25 %. Tensile strength was also evaluated. For more information regarding basics of Digital Image Correlation-technique, please refer to further literature.^[52]

2.8. Thermogravimetric Analysis (TGA)

Thermogravimetric analysis experiments were conducted using a TA Instruments Q5000 analyzer. The samples were heated from 30 to 600 °C at a rate of 10 K min⁻¹ in an argon atmosphere.

2.9. Attenuated Total Reflection Fourier Transformed Infrared Spectroscopy (ATR-FTIR)

ATR-FTIR measurements were performed on a Bruker Vertex70v ATR-IR spectrometer at room temperature in absorption mode.

2.10. Mass Spectrometry (GC-MS, ESI HRMS)

Gas chromatographic/mass spectroscopic analyses (GC-MS) were measured in DCM solutions using an Agilent GC 7890B equipped with HP-5MS UI columns (0.25 mm, 0.25 μm) and an MS 5977A single quadrupole mass detector. Samples were present at a concentration of 0.5 mg mL⁻¹. The temperature range of the chromatography was between 45 and 325 °C.

Electron-Spray High Resolution Ionization Mass Spectrometry (ESI HRMS) was measured on a Thermo Fisher Scientific Exactive Plus in negative mode in HPLC acetonitrile at a sample concentration of 1 ng mL⁻¹.

3. Results and Discussion

3.1. Epoxy Monomer Synthesis

EGCHC (5) epoxy monomer was prepared following the four-step synthesis shown in Figure 1 starting from sorbic acid (1). In an acid-catalyzed esterification reaction of sorbic acid (1) with allyl alcohol, allyl sorbate (2) was obtained. (2) is literature known but usually approached either by a reduction of the corresponding allyl 2-hexynoate with triphenylphosphine,^[53,54] an esterification reaction of allyl alcohol with the corresponding sorbic acid chloride^[55] or sorbic acid and allyl bromide or chloride.^[56] All of these reactions have drawbacks regarding their ecological footprint and toxicity because of the utilization of phosphines, bromides, or chlorides. The acid-mediated esterification used in this work in contrast is more favorable since it allows to use allyl sorbate and allyl alcohol as starting materials and sulfuric acid is only used as a catalyst in low concentrations. An additional advantage is the formation of water as a condensation product during the reaction instead of corrosive gases such as hydrogen chloride making additional scavenging steps unnecessary. Another benefit are comparable high yields up to 82 % in the esterification which can compete or outperform mentioned alternatives. A side reaction could be identified in an intramolecular Diels–Alder reaction of the vinyl- and allyl-group which is also described by Martin *et al.* but usually occurs at far higher temperatures than used in this work.^[55] Sorbic acid as starting material is a bio-molecule occurring in rowanberry oil and its very low mammalian toxicity makes its utilization as a food preservative possible.^[57,58] Allyl alcohol on the other hand is also bio-available by treating glycerin with formic acid or using catalytic synthesis methods.^[59,60] Successful preparation of allyl sorbate could be confirmed by NMR-spectroscopy (Figure S1; Figure S2, Supporting Information) and the spectral data were in agreement with those reported.^[55]

The next reaction step following the pathway in Figure 1 includes a Diels–Alder reaction between allyl sorbate and maleic anhydride forming the basic framework of the later epoxy compound. The high atom efficiency, reaction speed, and the access to complex molecular structures make the [4+2]-cycloaddition an appealing candidate for a greener approach toward epoxy resins. Maleic anhydride is a basic chemical with high industrial importance and it is known as a highly reactive dienophile while showing a relatively low environmental risk potential.^[61–63] Typically, it is produced by catalytic oxidation of hydrocarbons such as benzene in the gas phase.^[64] Recent publications though are focusing on renewable feedstocks such as furfural and its derivatives which can be gained out of carbohydrates.^[65–68] The Diels–Alder reaction can be performed in high concentrations (10 M referred to allyl sorbate) only requiring minimal amounts of solvent. As a further improvement, a solvent-free method utilizing microwave radiation as Moreno *et al.* proposed is conceivable.^[61] Successful synthesis of AHIBC (3) could be confirmed after crystallization and washing of the crude product by ¹H- and ¹³C-NMR spectroscopy (Figure 2A; Figure S3, Supporting Information, GC-MS Figure S4, Supporting Information) and elemental analysis.

The second allylation reaction leading to TACHC (4) is performed analog to the allylation of sorbic acid using H₂SO₄ as a catalyst. In this step, two allyl ester bonds are formed opening the anhydride introduced during the Diels–Alder cycloaddition. Full conversion could be confirmed by ¹H- and ¹³C-NMR spectroscopy (Figure 2B; Figure S5, Supporting Information), GC-MS (Figure S6, Supporting Information), and elemental analysis.

Finally, the oxidation of TACHC (4) was accomplished by a *Prilezhaev* reaction with *meta*-chloroperoxybenzoic acid (*mCPBA*) in dichloromethane at room temperature to yield 78 % within 48 h. Reaction progress can be easily monitored by the vanishing signals of the double bonds by ¹H-NMR. The amount of *mCPBA* seems to be high with 8 equivalents but considering the purity of the peroxy acid only being 77 % results in 1.5 equivalents per double bond. The ratios could be further improved by using hydrogen peroxide to regenerate the active species during the epoxidation reaction. An attractive alternative to substitute *mCPBA* could be found in the use of Oxone as the oxidizing agent in combination with acetone which reacts *in situ* to dimethylloxirane. Oxone refers to the triple salt 2KHSO₅ · KHSO₄ · K₂SO₄ and is widely used as an oxidizing agent in literature and is described as rather green, highly selective and catalyst free while being cheap and easy for storage.^[69–72] Here, the reaction proceeds much slower and usually takes up to three days to show full conversion in NMR which was the reason why the *mCPBA* path was the preferred synthesis route. Another green method to epoxidize allylic compounds which could possibly be transferred to the substrate produced in this work was reported by Aouf *et al.* using a chemo-enzymatic method.^[73] The successful synthesis of EGCHC (5) could be confirmed by ¹H- and ¹³C-NMR spectroscopy (Figure 2C; Figure S7, Supporting Information), and HRMS.

3.2. Curing of EGCHC

The curing conditions for EGCHC-based samples were chosen after DSC investigations. The onset temperature of the curing

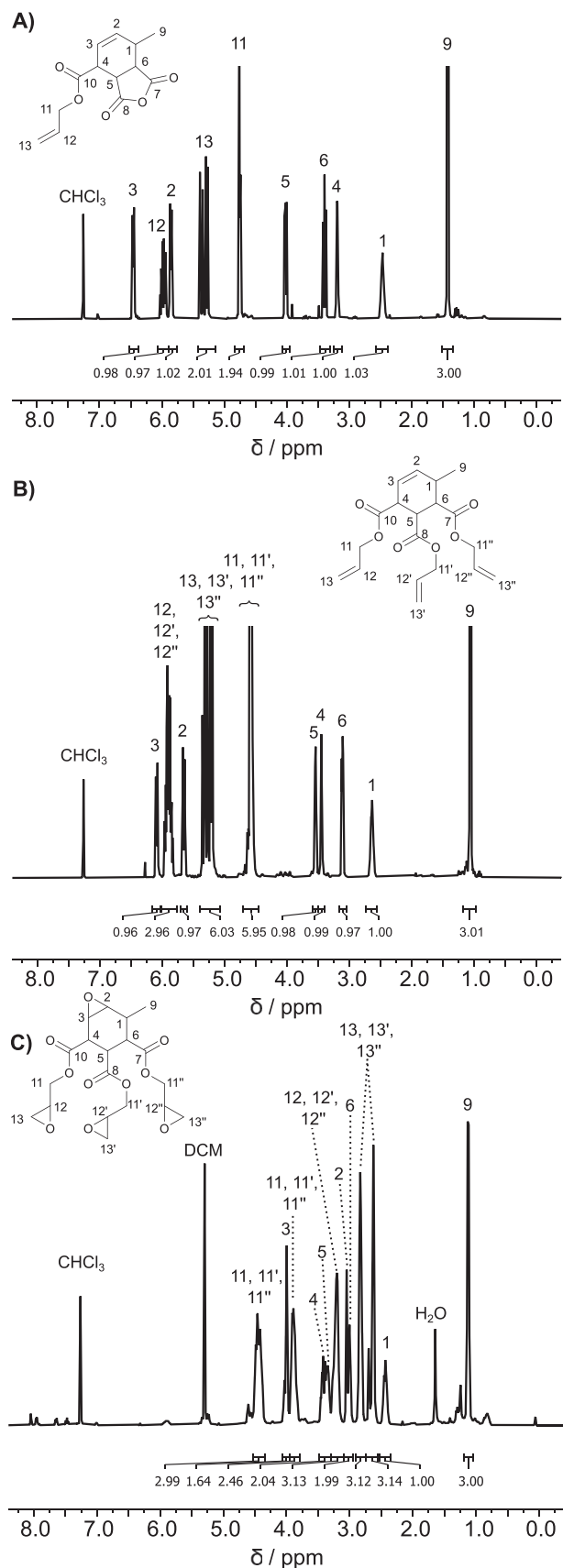


Figure 2. $^1\text{H-NMR}$ of the products: A) the Diels–Alder reaction (3), B) the allylation (4), and C) the epoxidation (5).

Table 4. Onset temperature of the curing enthalpy and temperature at the maximum of the exothermic peak.

Sample	Onset temperature in $^{\circ}\text{C}$	Maximum of the exothermic peak in $^{\circ}\text{C}$
EGCHC-IPD	43 ± 3	78 ± 1
EGCHC-T403	53 ± 3	94 ± 2
DGEBA-IPD	87 ± 3	121 ± 1
DGEBA-T403	103 ± 1	140 ± 1

Table 5. Gel-contents of the cured samples determined by Soxhlet-extraction with acetone as solvent. Extraction time: 24 h.

Sample	Gel-content in %
EGCHC-IPD	97.90 ± 0.95
EGCHC-T403	97.59 ± 0.15

enthalpy was set as the curing temperature. A temperature higher than the temperature of the maximum of the exothermic peak was chosen as the post-curing temperature. (Table 4) For the DGEBA-based samples, curing procedures similar to those described in the literature were used.^[48,49] The completion of the curing reaction was investigated with non-isothermal DSC measurements. Cured samples were subjected to a heating ramp (10 K min^{-1}) from -20 to 180°C . The cured EGCHC and DGEBA-based samples didn't show any residual exothermic reaction. Furthermore, the obtained Soxhlet gel-contents (Table 5) for EGCHC samples were high and justifies the curing conditions applied. The completion of the curing reaction could also be confirmed by ATR-IR measurements as no residual IR-bands of the C–O epoxide vibration at a wavelength of 820 cm^{-1} could be found (Figure S8, Supporting Information). Generally, the EGCHC thermograms show a higher reactivity than DGEBA as the onset temperature of the curing enthalpy and the temperature of the maximum of the exothermic peak are lower when curing with T403 and IPD (Figure 3). This could be confirmed by the lower activation energy found for EGCHC compared to DGEBA (see Table S1). An explanation for this can be found in the structure of the epoxy function in close distance to the ester. Due to inductive effects the ring-opening of the oxirane is facilitated and needs less energy to initiate the curing reaction. Jeffamine T403 itself can be considered as less reactive compared to IPD because of the sterical hindrance of the methyl groups in α position to the amine.^[74] The high reactivity of EGCHC allows a rapid completion of curing with moderate curing temperatures, which can be beneficial for saving energy.

3.3. Thermo-Mechanical Properties

Dynamic mechanical analysis (DMA) is an excellent method to determine the T_g of epoxy materials as it is a very sensitive technique.^[75] It also allows to compare the stiffness of the material at various temperatures. Figure 4 compares the storage modulus and $\tan \delta$ curves obtained with EGCHC and DGEBA cured with IPD and T403. As expected, the samples cured with IPD are stiffer and T_g is higher than the samples cured with T403.

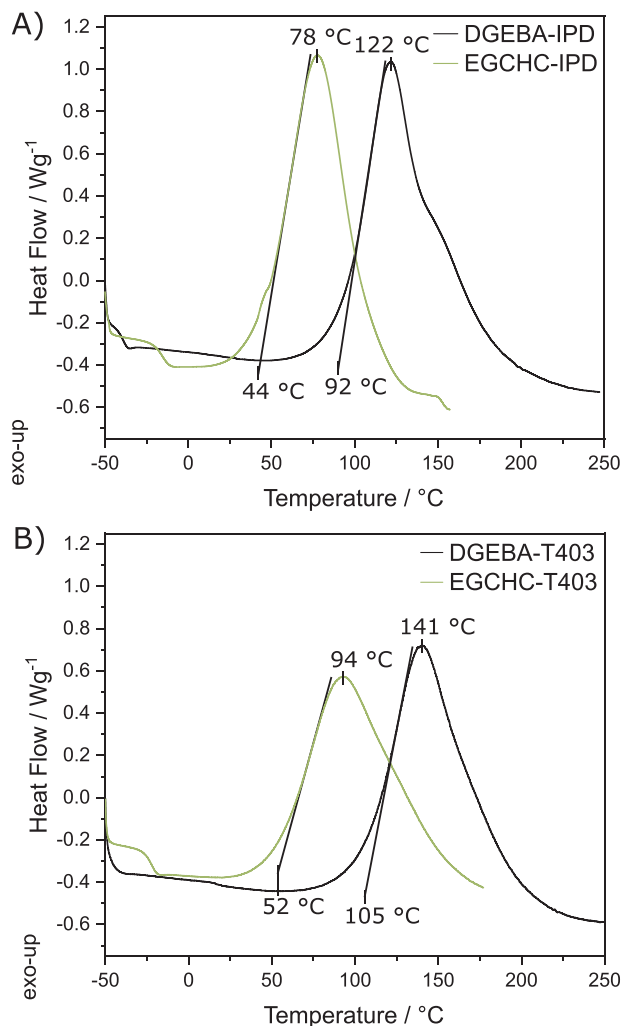


Figure 3. DSC scans of EGCHC/DGEBA-IPD A) and EGCHC/DGEBA-T403 B) with the onset temperature of the curing enthalpy and the temperature of the maximum of the exothermic peak.

The cycloaliphatic structure of IPD allows the creation of a more rigid network. Hence, IPD is better suited than T403 for applications that requires high stiffness at high temperatures. Between $-20\text{ }^{\circ}\text{C}$ and approximately $38\text{ }^{\circ}\text{C}$, EGCHC-T403 has a higher stiffness than DGEBA-T403. EGCHC-IPD has a higher stiffness than DGEBA-IPD between $-20\text{ }^{\circ}\text{C}$ and approximately $100\text{ }^{\circ}\text{C}$. Due to the large amount of oxirane rings in its structure, EGCHC has the ability to create a more dense crosslinked structure than DGEBA. However, the T_g of the EGCHC-based systems is lower than their DGEBA counterparts (Table 6). This can be explained by the structural differences of the resins. In contrast to EGCHC, DGEBA has aromatic substructures which can form the relatively strong intermolecular $\pi - \pi$ interactions. As a result, the glassy region for the EGCHC systems ends at lower temperatures than for the DGEBA systems and a rapid loss of stiffness is observed at lower temperatures. Nevertheless, EGCHC can still be used in applications that requires high temperatures as EGCHC-IPD shows a T_g of $130\text{ }^{\circ}\text{C}$ and no significant decrease of stiffness is observed between -20 and $100\text{ }^{\circ}\text{C}$.

Table 6. T_g obtained from DMA for the EGCHC and DGEBA-based samples.

Sample	T_g in $^{\circ}\text{C}$
EGCHC-IPD	129.8 ± 6.2
EGCHC-T403	56.5 ± 1.3
DGEBA-IPD	161.7 ± 0.4
DGEBA-T403	82.0 ± 1.2

3.4. Mechanical Properties

Figures 5 and 6 depict the tensile strength and tensile Modulus obtained for the DGEBA and EGCHC samples. As for DGEBA, EGCHC shows better mechanical properties when cured with IPD. A maximum average tensile modulus of 3965 MPa and a maximum average tensile strength of 76 MPa were found for the EGCHC-IPD specimens.

The results of tensile modulus are in accordance with the DMA results shown in Figure 4. EGCHC systems show a higher stiffness than the DGEBA-based epoxies and the samples cured with IPD are also stiffer than samples cured with T403. DGEBA is the most known epoxy resin and finds application in various domains. The higher E-modulus obtained with EGCHC underlines the capacity of EGCHC being able to have the required stiffness for high-performance applications. As an example, the product Biresin CR80 from SIKA is a epoxy system suitable for high-performance applications such as fibre reinforced composites parts for the marine, wind turbine and general industrial composite areas and reaches a tensile modulus of $2900\text{--}3000\text{ MPa}$ after curing.^[8] The tensile strength found for the DGEBA specimens are close to values reported in literature.^[48] EGCHC cured with IPD presents a high uncertainty on the tensile strength. As EGCHC-IPD sets within minutes at room temperature, the mixture could only be degassed for 30 s and not all the air inclusions could be removed. The presence of voids in the material after curing strongly affects the tensile strength. However, the average tensile strength of EGCHC-IPD is still higher than for DGEBA-IPD. EGCHC-T403 presents a similar tensile strength than DGEBA-T403. Thus, the results show that EGCHC can compete with the mechanical properties of DGEBA.

3.5. Thermal Stability

Thermal degradation of EGCHC-samples starts at temperatures of $203\text{ }^{\circ}\text{C}$ (IPD) and $222\text{ }^{\circ}\text{C}$ (T403) (Figure S9, Supporting Information). Even though the thermal stability of EGCHC is lower than DGEBA (around $340\text{ }^{\circ}\text{C}$), the $T_{5\%}$ of both EGCHC-IPD and EGCHC-T403 is high enough to not degrade the material under usage in standard applications. The lower thermal stability of EGCHC samples can be attributed to the ester bonds which are more prone to pyrolysis compared to ether bonds present in DGEBA and to the absence of aromatic substructures.

3.6. Solvolysis of EGCHC-Based Thermosets

The dissolving of polymers in solvents is of high interest in various domains.^[77] For example, in the fiber-reinforced polymers

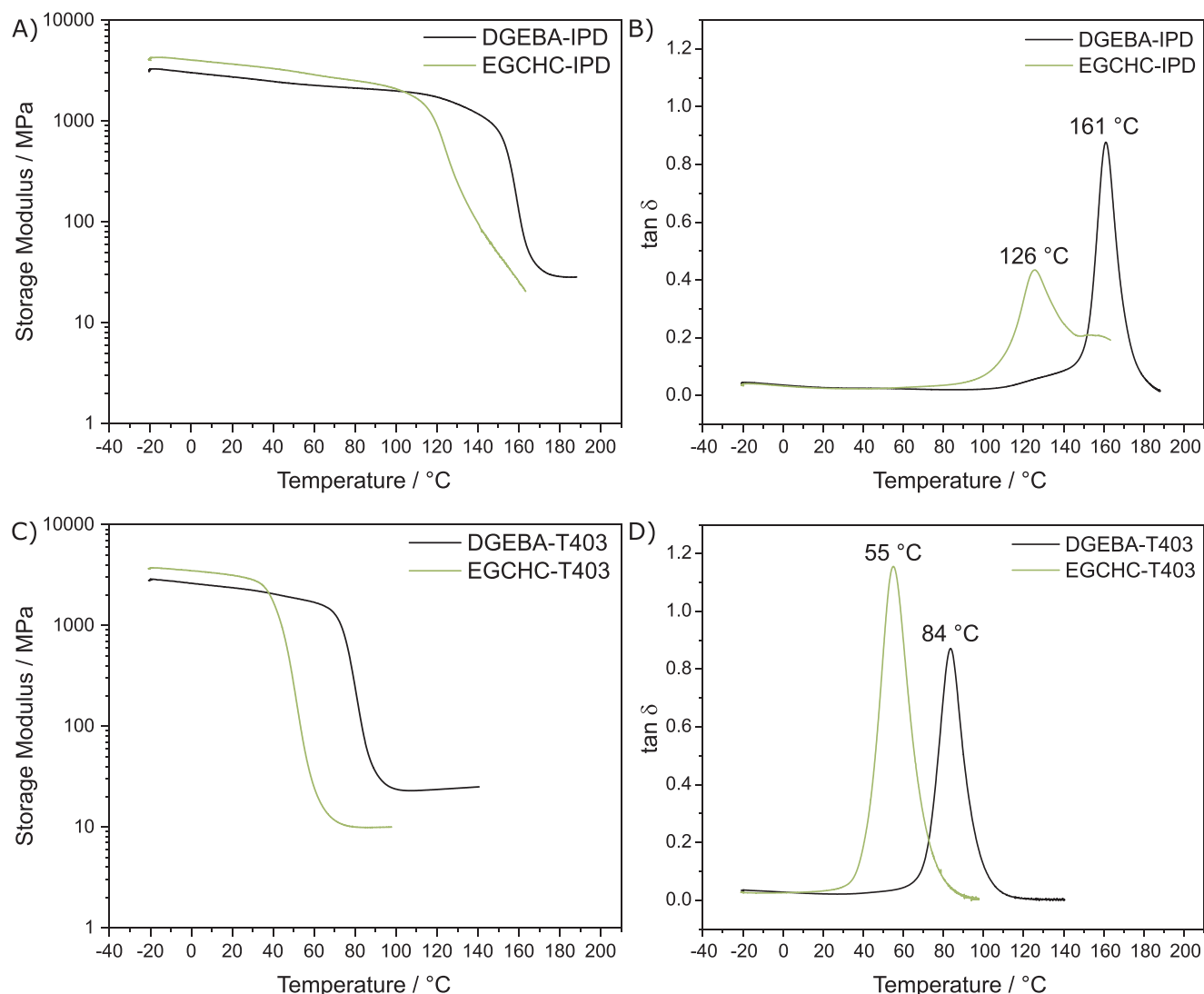


Figure 4. A) Storage modulus and B) $\tan \delta$ of DGEBA/EGCHC cured with IPD, C) Storage modulus and D) $\tan \delta$ of DGEBA/EGCHC cured with T403. Determined by DMA.

industry, being able to dissolve the polymer matrix would allow an easy recovery of the fibers. Fibers, especially carbon fibers are costly materials due to the complex and energy-intensive production process. In contrast to DGEBA, the resin presented in this paper contain ester groups which can undergo basic hydrolysis. Normally, dense crosslinked thermosets are only dissolvable by applying harsh conditions such as high temperatures or pressure.^[77-79] In order to investigate the solvolysis behaviour of EGCHC-based epoxy resins samples were placed into a 1 M NaOH solution and the degradation at 80 °C and room temperature were evaluated. At 80 °C, both samples cured with IPD and Jeffamine T403 dissolved within 30 min. At room temperature, the sample EGCHC+T403 decomposed completely over the time of 17 h (Figure S10, Supporting Information) The sample EGCHC+IPD was more persistent and lost 17 % of its original weight. It takes about 4 d until complete solvolysis (Figure 7). This different behaviour can be explained with the density of the 3D-network. Jeffamine T403 is build of repeating oxypropylene

units in its backbone which results in larger gaps in the cured structure. This then allows the solvent deeper penetration and attacking the ester bonds. Compared to this the network formed by curing with IPD is more dense allowing less degrees of freedom hindering the solvent to diffuse into the thermoset.

3.7. Ecological Assessment

The assessment of the ecology of the complete reaction synthesis is evaluated using the bio-based fraction of the product. Therefore, each component is analyzed with regard to the bio-based content of substances available in industrial scale. Furthermore, different scenarios are displayed showing the development of the bio-based content using published routes to synthesize the different educts with renewable resources. Hence, both a conservative approach and an optimistic development of the availability of renewable chemicals is looked at for the epoxy EGCHC. Further-

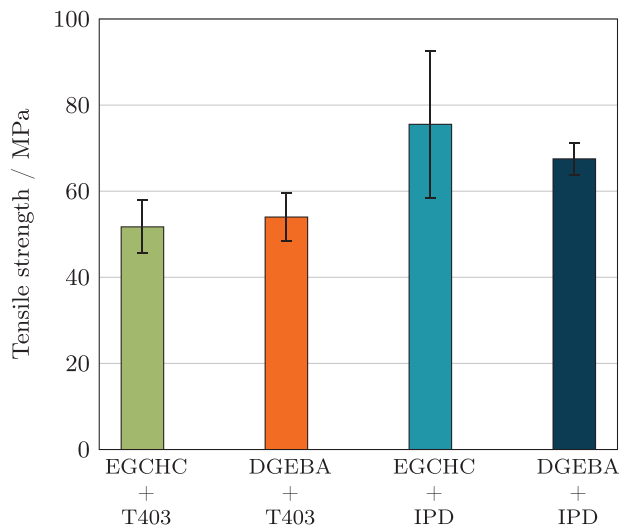


Figure 5. Tensile strength of EGCHC-IPD, EGCHC-T403, DGEBA-IPD, and DGEBA-T403.

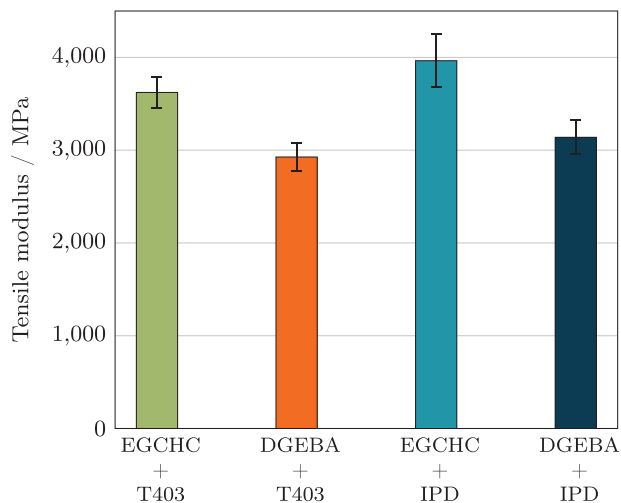


Figure 6. Tensile modulus of EGCHC-IPD, EGCHC-T403, DGEBA-IPD, and DGEBA-T403.

more, a comparison is drawn with the industry standard DGEBA both pure and cured with standard curing agents. Bio-based fractions are calculated according to the structural information of the molecules and their change throughout the reaction as reported in the standard DIN EN 16785-1.^[80] This method thoroughly determines the bio-based fraction with radiocarbon and elemental analysis by taking the total content of bio-originating H, C, O, and N atoms into consideration. The bio-based content w_{bb} represents the mass fraction of the bio-based mass m_{HCON} (total H, C, O, N mass) in relation to the total sample mass m . Additionally, the bio-based carbon content is reported according to norm ASTM D6866.^[81]

3.7.1. Synthesis Route

As stated previously, allyl alcohol is readily bio-available.^[59,60] Allyl sorbate which is synthesized from sorbic acid and allyl alcohol

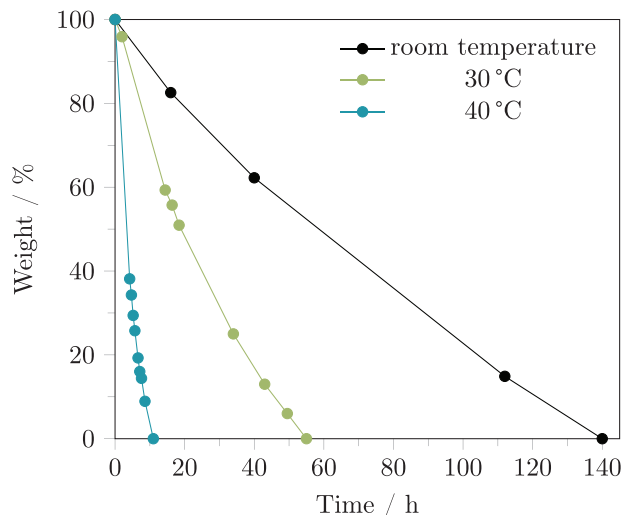


Figure 7. Decomposition of EGCHC-IPD in 1 M NaOH at room temperature, 30 and 40 °C.

is calculated to contain a bio-based fraction of $w_{bb} = 0.753$. Sorbic acid is in theory available as a natural resource from rowan berries.^[57,82] Though, the current industrial relevant route is the condensation of malonic acid (fossil) and crotonaldehyde (100 % bio-based),^[83-85] described by Doebner.^[86] Therefore, a conservative fraction of $w_{bb} = 0.667$ is assumed for sorbic acid. The second reaction step involving allyl sorbate and maleic anhydride reduces the bio-based content of the intermediate to 45.8 %. Maleic anhydride is produced in large amounts mostly from butane oxidation.^[64,87,88] Due to the importance of maleic anhydride as a building block in the chemical industry more and more green synthesis routes are published,^[65,89-92] though none has yet been implemented in an industrial scale. TACHC which is formed via an addition and condensation of two allyl alcohol molecules increases the bio-based fraction again to $w_{bb} = 0.630$. For the final epoxidation step the reaction pathway using *m*CPBA is taken as the underlying synthesis route. The peroxy-carboxylic acid is a commercially available oxidizing agent which is industrially prepared using fossil resources.^[93] Hence, three oxygen atoms are inserted into TACHC forming the final product EGCHC with a bio-based content of $w_{bb} = 0.532$. Applying the same methodology with the standard ASTM D6866 results in a bio-based fraction of 68.4 % as only carbon atoms are tracked with this method.^[81] Substituting some of the conventional produced chemical components with bio-based alternatives could further increase the total bio-based content.

3.7.2. Comparison of EGCHC and DGEBA

Figure 8 shows the conservative calculation of the bio-based content of EGCHC with currently available green chemicals using both aforementioned standard in comparison with the standard epoxy DGEBA. Depending on the underlying norm, different bio-based fractions can be determined, whereby EGCHC scores largely improved bio-based contents as its conventional competitor. For DGEBA the best case scenario is applied, which assumes a synthesis of BPA and 100 % green epichlorohydrin.

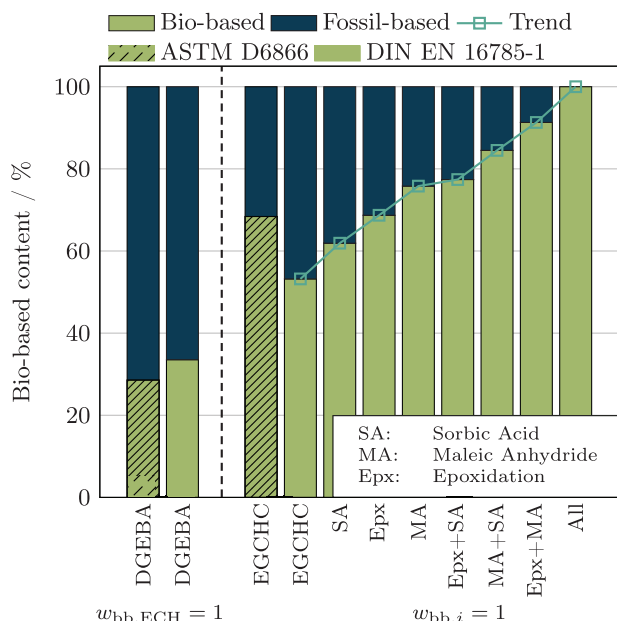


Figure 8. Bio-based content of EGCHC in comparison with DGEBA calculated using the standard DIN EN 16785-1^[81] and ASTM D6866.^[82] Development of the bio-based content with substitution of fossil-based components for EGCHC. Bio-based content of DGEBA systems from assumed 100 % green epichlorohydrine.

Nevertheless, due to its small molecular weight, the bio-based content of DGEBA can thereby only be increased to $w_{bb} = 0.335$. Furthermore, the problems arising with the toxicity of the used chemicals, as stated in the introductory section, are still present.

3.7.3. Scenarios for Increasing Bio-Based Fraction of EGCHC

Figure 8 also depicts different scenarios which illustrate the development of the bio-based fraction by using green alternatives in the here proposed production of EGCHC. As it can clearly be seen, a vast improvement in greenness can be achieved without changing the synthesis route. Feasible options for producing bio-based sorbic acid and maleic anhydride are known and reported in literature which are as in most cases hindered by the more cost effective conventional processes. Though, with increasing demands for bio-based products this could change in the near future. Hence, steps to 61.9 %, 75.8 %, and 84.5 % can easily be achieved in the scenario of 100 % bio-based sorbic acid, maleic anhydride or both, respectively.

The epoxidation step is more challenging to replace as there are to our knowledge no reported routes for bio-based *m*CPBA. Therefore, the logic consequence would be to take another epoxidation method into consideration as stated in section 3.1. Further green alternatives to *m*CPBA comprise hydrogen peroxide in combination with different catalysts ranging from polyoxometalates,^[94,95] Pt,^[96] methyltrioxorhenium^[97] or enzymes.^[73,98-100] Testing various alternative reactions showed to be either very slow or the terminal double bonds could not be epoxidized at all. Nevertheless, an alternative route comprising bio-based educts, for example, with enzymes, would increase the total bio-based content by 15.5 % to 68.7 % taking the initial value

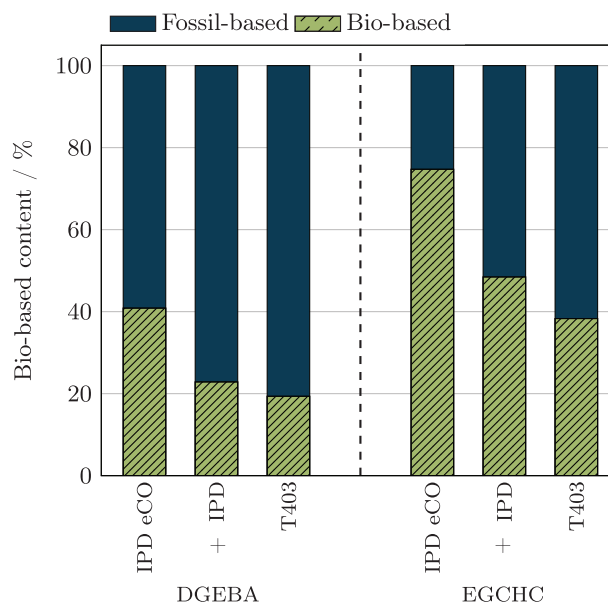


Figure 9. Bio-based content of resins cured with IPD eCO, IPD and T403 of EGCHC in comparison with DGEBA calculated using the standard ASTM D6866.^[82] Bio-based content of DGEBA stems from assumed 100 % green epichlorohydrine.

of $w_{bb} = 0.532$ as a base. It is to be noted that for ASTM D6866 the epoxidation step does not influence the bio-based fraction as oxygen atoms are not included in the determination.

3.7.4. Curing of EGCHC and DGEBA

The synthesized epoxy EGCHC which was cured with both IPD and T403 will also be compared with the industrial relevant competitor DGEBA. **Figure 9** illustrates the different achievable bio-based contents for the four resin systems calculated with standard ASTM D6866. For IPD two cases are considered. Either using conventional fossil-based IPD or readily available green IPD (VESTAMIN IPD eCO), available with a 90 % bio-based carbon content.^[102] Due to the different required mixing ratios, the influence of the epoxy is more or less pronounced. Nevertheless, for all studied samples an increased bio-based fraction can be observed which has no impact on the material strength as shown before. For the sampled cured with IPD a total bio-based content of $w_{bb} = 0.268$ and $w_{bb} = 0.377$ can be calculated for DGEBA and EGCHC, respectively. Substituting IPD with IPD eCO leads to the highest bio-based contents. Considering a current standard system of DGEBA cured with IPD, a maximum bio-based carbon amount can be achieved by using both green ECH ($w_{bb} = 1$) in combination with ECO IPD ($w_{bb} = 0.9$). As a result an epoxy resin with a total bio-based carbon content of 40.9 % can be synthesized which, however, still relays on the use of BPA. In contrast to that, a resin produced with EGCHC and IPD eCO outperforms the state of the art DGEBA-system by more than 33 % adding up to $w_{bb} = 0.747$. This sets a new benchmark in the green epoxy resin market in the field of low-temperature applications.

4. Conclusion

Bio-based epoxy resins often suffer from the comparison with petrochemical-based epoxies as their mechanical properties are rather poor. However, the values of the tensile E-modulus and tensile strength found for the EGCHC-specimens show that the mechanical properties of EGCHC can compete with DGEBA. With its high amount of oxirane groups, EGCHC can form, when cured with conventional amine hardeners, cross-linked networks which exhibit high stiffness and high strength. Better mechanical properties and higher T_g were found when EGCHC was cured with IPD. Furthermore, the presence of ester bonds allows EGCHC solvolysis in NaOH in very mild conditions which makes it a particular interesting material for the composite industry as it would allow an easy recovery of the fibers at the end-of-life of a composite component. A significant bio-based content of 68.4 % is readily achieved for EGCHC resin and can reach 74.7 % when cured with green IPD. The high bio-based content of EGCHC additionally with its BPA and ECH-free nature, makes EGCHC a promising alternative to conventional epoxy thermosets.

Supporting Information

Supporting Information is available from the Wiley Online Library or from the author.

Acknowledgements

J.M.B. and N.R. contributed equally to this work. The authors would like to thank Moritz Kränzlein for his help with NMR interpretation, Philipp Weingarten for HR-MS measurements as well as Peter Bramberger for his enthusiasm in the initial phase of the project. The funding by the German Federal Ministry of Education and Research (BMBF) for the “Green Carbon” project (FKZ: 03SF0577A) was gratefully acknowledged.

Open access funding enabled and organized by Project DEAL.

Conflict of Interest

The authors declare no conflict of interest.

Data Availability Statement

The data that support the findings of this study are available in the supplementary material of this article.

Keywords

bio-based materials, epoxy thermosets, sorbic acid, thermo-mechanical properties

Received: February 27, 2023

Revised: April 5, 2023

Published online: May 18, 2023

[1] N. Prilezhaev, *Ber. Dtsch. Chem. Ges.* **1909**, 42, 4811.

[2] X. M. Chen, B. Ellis, in, *Chemistry and Technology of Epoxy Resins*, Springer, Dordrecht, **1993**, pp. 303–325.

- [3] H. Jin, G. M. Miller, S. J. Pety, A. S. Griffin, D. S. Stradley, D. Roach, N. R. Sottos, S. R. White, *Int. J. Adhes. Adhes.* **2013**, 44, 157.
- [4] C.-H. Park, S.-W. Lee, J.-W. Park, H.-J. Kim, *React. Funct. Polym.* **2013**, 73, 641.
- [5] F.-L. Jin, X. Li, S.-J. Park, *J. Ind. Eng. Chem.* **2015**, 29, 1.
- [6] X. Wang, W. Guo, L. Song, Y. Hu, *Compo., Part B* **2019**, 179, 107487.
- [7] N. J. Jin, J. Yeon, I. Seung, K.-S. Yeon, *Constr. Build. Mater.* **2017**, 156, 933.
- [8] Sika Deutschland GmbH, “Biresin CR80 Compositeharz-System”, can be found under <https://industry.sika.com/content/dam/dms/deaddconst01/x/PDB-Biresin-CR80-inkl-DNV-GL-de.pdf>, **2021**.
- [9] E. A. Baroncini, S. Kumar Yadav, G. R. Palmese, J. F. Stanzione, *J. Appl. Polym. Sci.* **2016**, 133, 44103.
- [10] J. C. Fishbein, J. M. Heilman, (Eds.), *Advances in Molecular Toxicology*, Elsevier, Amsterdam, **2015**.
- [11] K. Hąc-Wydro, K. Poleć, M. Broniatowski, *J. Mol. Liq.* **2019**, 289, 111136.
- [12] K.-A. Hwang, K.-C. Choi, In J. C. Fishbein, J. M. Heilman, (Eds.), *Advances in Molecular Toxicology*, Vol. 9, Elsevier, Amsterdam, ISBN 1872-0854, **2015**, pp. 1–33.
- [13] M. R. Loos, L. A. F. Coelho, S. H. Pezzin, S. C. Amico, *Polímeros* **2008**, 18, 76.
- [14] R. A. Nowak, F. Koohestani, J. Bi, P. Mehrotra, F. S. Mesquita, F. Masoud, S. A. Machado, *Comprehensive Toxicology* 2nd ed. Elsevier, Amsterdam, ISBN 978-0-08-046884-6, **2010**, pp. 499–522.
- [15] W. H. Lawrence, M. Malik, J. E. Turner, J. Autian, *J. Pharm. Sci.* **1972**, 61, 1712.
- [16] X. Su, Z. Zhou, J. Liu, J. Luo, R. Liu, *Eur. Polym. J.* **2020**, 140, 110053.
- [17] A. S. Amarasekara, R. Garcia-Obergon, A. K. Thompson, *J. Appl. Polym. Sci.* **2019**, 136, 47000.
- [18] S. Caillol, B. Boutevin, R. Auvergne, *Polymer* **2021**, 223, 123663.
- [19] I. Faye, M. Decostanzi, Y. Ecochard, S. Caillol, *Green Chem.* **2017**, 19, 5236.
- [20] C. Gioia, M. Colonna, A. Tagami, L. Medina, O. Sevastyanova, L. A. Berglund, M. Lawoko, *Biomacromolecules* **2020**, 21, 1920.
- [21] S. Kumar, S. K. Samal, S. Mohanty, S. K. Nayak, *Polym.-Plast. Technol. Eng.* **2018**, 57, 133.
- [22] D. Matykievicz, K. Skórczewska, *Materials* **2022**, 15, 14.
- [23] H. Nabipour, H. Niu, X. Wang, S. Batool, Y. Hu, *React. Funct. Polym.* **2021**, 168, 105034.
- [24] S. Nikafshar, O. Zabihi, S. Hamidi, Y. Moradi, S. Barzegar, M. Ahmadi, M. Naebe, *RSC Adv.* **2017**, 7, 8694.
- [25] Z. Wang, P. Gnanasekar, S. Sudhakaran Nair, R. Farnood, S. Yi, N. Yan, *ACS Sustainable Chem. Eng.* **2020**, 8, 11215.
- [26] X. Zhen, H. Li, Z. Xu, Q. Wang, S. Zhu, Z. Wang, Z. Yuan, *Int. J. Biol. Macromol.* **2021**, 182, 276.
- [27] D. Santiago, D. Guzmán, X. Ramis, F. Ferrando, À. Serra, *Polymers* **2019**, 12, 44.
- [28] J. Xin, M. Li, R. Li, M. P. Wolcott, J. Zhang, *ACS Sustainable Chem. Eng.* **2016**, 4, 2754.
- [29] J. Xin, P. Zhang, K. Huang, J. Zhang, *RSC Adv.* **2014**, 4, 8525.
- [30] T. Koike, *Polym. Eng. Sci.* **2012**, 52, 701.
- [31] D. Fourcade, B. S. Ritter, P. Walter, R. Schönfeld, R. Mülhaupt, *Green Chem.* **2013**, 15, 910.
- [32] P. Niedermann, G. Szebenyi, A. Toldy, *Express Polym. Lett.* **2015**, 9, 85.
- [33] M. Chrysanthos, J. Galy, J.-P. Pascault, *Polymer* **2011**, 52, 3611.
- [34] J. Łukaszczuk, B. Janicki, M. Kaczmarek, *Eur. Polym. J.* **2011**, 47, 1601.
- [35] Z. Rapi, B. Szolnoki, P. Bakó, P. Niedermann, A. Toldy, B. Bodzay, G. Keglevich, G. Marosi, *Eur. Polym. J.* **2015**, 67, 375.
- [36] European Commission. Joint Research Centre, BTG Biomass Technology Group B.V., *Insights into the European market for bio-based chemicals: factsheets for 10 biobased product categories*, Publications Office, Luxembourg, **2019**.

- [37] B. M. Bell, J. R. Briggs, R. M. Campbell, S. M. Chambers, P. D. Gaarenstroom, J. G. Hippler, B. D. Hook, K. Kearns, J. M. Kenney, W. J. Kruper, D. J. Schreck, C. N. Theriault, C. P. Wolfe, *Clean: Soil, Air, Water* **2008**, 36, 657.
- [38] G. M. Lari, G. Pastore, C. Mondelli, J. Pérez-Ramírez, *Green Chem.* **2018**, 20, 148.
- [39] S. M. Danov, O. A. Kazantsev, A. L. Esipovich, A. S. Belousov, A. E. Rogozhin, E. A. Kanakov, *Catal. Sci. Technol.* **2017**, 7, 3659.
- [40] N. W. Manthey, F. Cardona, G. Francucci, T. Aravinthan, *J. Compos. Mater.* **2014**, 48, 1611.
- [41] R. Mustapha, A. R. Rahmat, R. Abdul Majid, S. N. H. Mustapha, *Polym.-Plast. Technol. Mater.* **2019**, 58, 1311.
- [42] T. S. Omonov, J. M. Curtis, *J. Appl. Polym. Sci.* **2014**, 131, 8.
- [43] N. Reinhardt, J. M. Breitsamer, K. Drechsler, B. Rieger, *Macromol. Mater. Eng.* **2022**, 307, 2200455.
- [44] A. Anusic, Y. Blöchl, G. Oreski, K. Resch-Fauster, *Polym. Degrad. Stab.* **2020**, 181, 109284.
- [45] S. Malburet, C. Di Mauro, C. Noè, A. Mija, M. Sangermano, A. Graillot, *RSC Adv.* **2020**, 10, 41954.
- [46] A. Todorovic, K. Resch-Fauster, A. R. Mahendran, G. Oreski, W. Kern, *J. Appl. Polym. Sci.* **2021**, 138, 50239.
- [47] H. Behniafar, M. K. Nazemi, *Polym. Bull.* **2017**, 74, 3739.
- [48] H. Cai, P. Li, G. Sui, Y. Yu, G. Li, X. Yang, S. Ryu, *Thermochim. Acta* **2008**, 473, 101.
- [49] E. Ernault, Ph.D. thesis, Arts et Métiers, Paris, **2016**.
- [50] F. G. Garcia, B. G. Soares, V. J. R. R. Pita, R. Sánchez, J. Rieumont, *J. Appl. Polym. Sci.* **2007**, 106, 2047.
- [51] J. Wan, C. Li, Z.-Y. Bu, C.-J. Xu, B.-G. Li, H. Fan, *Chem. Eng. J.* **2012**, 188, 160.
- [52] M. A. Sutton, J.-J. Orteu, H. W. Schreier, in *Image Correlation for Shape, Motion and Deformation Measurements: Basic Concepts, Theory and Applications*, Springer, New York, NY **2009**.
- [53] B. M. Trost, U. Kazmaier, *J. Am. Chem. Soc.* **1992**, 114, 7933.
- [54] C. Guo, X. Lu, *J. Chem. Soc., Perkin Trans. 1* **1993**, 16, 1921.
- [55] S. F. Martin, S. A. Williamson, R. P. Gist, K. M. Smith, *J. Org. Chem.* **1983**, 48, 5170.
- [56] P. Klán, P. Beňovský, *Monatsh. Chem.* **1992**, 123, 469.
- [57] A. W. Hofmann, *Justus Liebig's Ann. Chem.* **1859**, 110, 129.
- [58] J. D. Piper, P. W. Piper, *Compr. Rev. Food Sci. Food Saf.* **2017**, 16, 868.
- [59] X. Li, Y. Zhang, *ACS Catal.* **2016**, 6, 143.
- [60] V. Canale, L. Tonucci, M. Bressan, N. d'Alessandro, *Catal. Sci. Technol.* **2014**, 4, 3697.
- [61] M. Moreno, M. V. Gomez, C. Cebrian, P. Prieto, A. de La Hoz, A. Moreno, *Green Chem.* **2012**, 14, 2584.
- [62] European Union, "Substance information - ECHA: Maleic anhydride", can be found under <https://echa.europa.eu/de/substance-information/-/substanceinfo/100.003.247>, **2022**.
- [63] G. Østergaard, E. Nielsen, O. Ladefoged, *Evaluation of health hazards by exposure to maleic anhydride and proposal of a health-based quality criterion for ambient air*, The Danish Environmental Protection Agency, Copenhagen, **2013**.
- [64] K. Lohbeck, H. Haferkorn, W. Fuhrmann, N. Fedtke, *Ullmann's Encyclopedia of Industrial Chemistry*, Wiley GmbH & Co. KGaA, Weinheim, Germany, ISBN 3527306730, **2000**.
- [65] Z. Du, J. Ma, F. Wang, J. Liu, J. Xu, *Green Chem.* **2011**, 13, 554.
- [66] H. Guo, G. Yin, *J. Phys. Chem. C* **2011**, 115, 17516.
- [67] S. Shi, H. Guo, G. Yin, *Catal. Commun.* **2011**, 12, 731.
- [68] H. Choudhary, S. Nishimura, K. Ebitani, *Appl. Catal., A* **2013**, 458, 55.
- [69] H. M. Ferraz, R. M. Muzzi, T. de O. Vieira, H. Viertler, *Tetrahedron Lett.* **2000**, 41, 5021.
- [70] S. E. Denmark, D. C. Forbes, D. S. Hays, J. S. DePue, R. G. Wilde, *J. Org. Chem.* **1995**, 60, 1391.
- [71] L. Charbonneau, X. Foster, S. Kaliaguine, *ACS Sustainable Chem. Eng.* **2018**, 6, 12224.
- [72] L. Charbonneau, X. Foster, D. Zhao, S. Kaliaguine, *ACS Sustainable Chem. Eng.* **2018**, 6, 5115.
- [73] C. Aouf, J. Lecomte, P. Villeneuve, E. Dubreucq, H. Fulcrand, *Green Chem.* **2012**, 14, 2328.
- [74] E. Darroman, N. Durand, B. Boutevin, S. Caillol, *Prog. Org. Coat.* **2016**, 91, 9.
- [75] S. Ebnesajjad, C. F. Ebnesajjad, in *Surface Treatment of Materials for Adhesion Bonding*, 2nd ed., William Andrew, ISBN 9780323264358, **2014**.
- [76] B. A. Miller-Chou, J. L. Koenig, *Prog. Polym. Sci.* **2003**, 28, 1223.
- [77] X. Kuang, Q. Shi, Y. Zhou, Z. Zhao, T. Wang, H. J. Qi, *RSC Adv.* **2018**, 8, 1493.
- [78] L. Henry, A. Schneller, J. Doerfler, W. M. Mueller, C. Aymonier, S. Horn, *Polym. Degrad. Stab.* **2016**, 133, 264.
- [79] R. Morales Ibarra, M. Sasaki, M. Goto, A. T. Quitain, S. M. García Montes, J. A. Aguilar-Garib, *J. Mater. Cycles Waste Manage.* **2015**, 17, 369.
- [80] R. Piñero-Hernanz, J. García-Serna, C. Dodds, J. Hyde, M. Poliakoff, M. J. Cocero, S. Kingman, S. Pickering, E. Lester, *J. Supercrit. Fluids* **2008**, 46, 83.
- [81] Din en 16785-1:2016-03, biobasierte produkte - biobasierter gehalt - teil 1: Bestimmung des biobasierten gehalts unter verwendung der radiokarbon- und elementaranalyse; deutsche fassung en 16785-1:2015.
- [82] D20 Committee, Test methods for determining the biobased content of solid, liquid, and gaseous samples using radiocarbon analysis.
- [83] E. Letzig, W. Handschack, *Nahrung* **1963**, 7, 591.
- [84] Godavari Biorefineries Ltd., Crotonaldehyde - 99%.
- [85] E. Lück, M. Jager, N. Raczek, in *Ullmann's Encyclopedia of Industrial Chemistry*, Wiley GmbH & Co. KGaA, Weinheim, Germany, ISBN 3527306730, **2000**.
- [86] E. d. J. Avantium, H. Stichnothe, G. Bell, H. Jorgensen, Bio-based chemicals: A 2020 Update", can be found under <https://www.ieabioenergy.com/blog/publications/new-publication-bio-based-chemicals-a-2020-update/>, **2020**.
- [87] O. Doebner, *Ber. Dtsch. Chem. Ges.* **1900**, 33, 2140.
- [88] J. C. Burnett, R. A. Keppel, W. D. Robinson, *Catal. Today* **1987**, 1, 537.
- [89] O. M. Musa, (Ed.), in *Handbook of Maleic Anhydride Based Materials: Syntheses, Properties and Applications*, Springer, Cham, **2016**.
- [90] R. Wojcieszak, F. Santarelli, S. Paul, F. Dumeignil, F. Cavani, R. V. Gonçalves, *Sustainable Chem. Processes* **2015**, 3, 1.
- [91] N. Alonso-Fagúndez, M. L. Granados, R. Mariscal, M. Ojeda, *ChemSusChem* **2012**, 5, 1984.
- [92] W. Jia, Z. Si, Y. Feng, X. Zhang, X. Zhao, Y. Sun, X. Tang, X. Zeng, L. Lin, *ACS Sustainable Chem. Eng.* **2020**, 8, 7901.
- [93] J. Lan, J. Lin, Z. Chen, G. Yin, *ACS Catal.* **2015**, 5, 2035.
- [94] T. Maki, K. Takeda, in *Ullmann's Encyclopedia of Industrial Chemistry*, Wiley GmbH & Co. KGaA, Weinheim, Germany, ISBN 3527306730, **2000**.
- [95] N. Mizuno, K. Yamaguchi, *Chem. Rec.* **2006**, 6, 12.
- [96] R. Fareghi-Alamdari, S. M. Hafshejani, H. Taghiyar, B. Yadollahi, M. R. Farsani, *Catal. Commun.* **2016**, 78, 64.
- [97] M. Colladon, A. Scarso, P. Sgarbossa, R. A. Michelin, G. Strukul, *J. Am. Chem. Soc.* **2007**, 129, 7680.
- [98] W. A. Herrmann, R. M. Kratzer, R. W. Fischer, *Angew. Chem., Int. Ed. Eng.* **1997**, 36, 2652.
- [99] E. Abdulmalek, M. Arumugam, H. N. Mizan, M. B. Abdul Rahman, M. Basri, A. B. Salleh, *Sci. World J.* **2014**, 2014, 1.
- [100] C. Aouf, E. Durand, J. Lecomte, M.-C. Figueroa-Espinoza, E. Dubreucq, H. Fulcrand, P. Villeneuve, *Green Chem.* **2014**, 16, 1740.
- [101] F. P. Cuperus, S. T. Bouwer, G. F. H. Kramer, J. T. P. Derksen, *Bio-catalysis* **1994**, 9, 89.
- [102] EVONIK, The eco portfolio: Performance meets sustainability.